Showa Univ J Med Sci **28**(2), 135～145, June 2016

Original

Quantification of (−)-Epigallocatechin-3-gallate Inhibition of Anaplastic Thyroid Cancer Cell Line Adhesion and Proliferation Using Real-time Cell Analysis

Masayuki MIYAZAWA[1,2], Shinichi IWAI*[1,3], Takeshi HAYASHI[1,2], Yuko UDAKA[1], Akiko SASAKI[1], Shotaro HASHIMOTO[1], Takehiko SAMBE[1], Kiyoshi FUKUHARA[4] and Katsuji OGUCHI[1]

Abstract: Anaplastic thyroid cancer (ATC) has a poor prognosis because of immediate metastasis. Several studies in humans and animals have suggested that the ingestion of green tea or its active ingredient (−)-epigallocatechin-3-gallate (EGCG) may decrease the risk of cancer. Using a recently developed real-time cell analysis (RTCA) system, we have shown previously that EGCG inhibits cell migration and the invasion of oral cavity cancers by suppressing matrix metalloproteinases. In the present study we used RTCA to investigate the effects of EGCG on cell adhesion to fibronectin-coated plates using three cancer cell lines: one ATC cell line (TCO-1) and two poorly differentiated oral squamous cell carcinomas (OSCCs) cell lines (SAS and HO-1-u-1; originating from the tongue and floor of the mouth, respectively). EGCG (50 μM) inhibited the adhesion of all three cell lines. In addition to its effects on cell adhesion, 50 μM EGCG inhibited the cell proliferation of TCO-1 cells. Furthermore, EGCG decreased α_V *integrin* (*ITGAV*) mRNA levels in all three cell lines, suggesting that EGCG inhibits the cell adhesion and proliferation of OSCC and ATC cells via suppression of integrin expression. Therefore, EGCG represents a useful dietary constituent or a lead compound for counteracting metastasis of oral cavity cancers and thyroid cancers.

Key words: anaplastic thyroid cancer, oral squamous cell carcinoma, adhesion, (−)-epigallocatechin-3-gallate (EGCG), real-time cell analyzer

Introduction

Green tea is consumed worldwide. Because it contains catechins, green tea may have therapeutic potential in areas such as preventing cancer[1], pollinosis[2], and osteoporosis[3]. There are four main catechins in green tea: (−)-epigallocatechin-3-gallate (EGCG), (−)-epigallocatechin, (−)-epicatechin-3-gallate, and (−)-epicatechin[4]. EGCG, the primary catechin in green tea,

[1] *Department of Pharmacology, Showa University School of Medicine,* 1-5-8 Hatanodai, Shinagawa-ku, Tokyo 142-8555, Japan.
[2] *Department of Otorhinolaryngology, Showa University School of Medicine.*
[3] *Department of Healthcare and Regulatory Sciences, Division of Pharmaceutical Regulatory Pharmacy, Showa University School of Pharmacy.*
[4] *Department of Medical Chemistry, Division of Organosynthetic Chemistry, Showa University School of Pharmacy.*
* To whom corresponding should be addressed.

exhibits strong activity in various assays, including antitumor, anti-oxidation, and anti-angiogenesis assays[5,6].

The xCELLigence real-time cell analysis (RTCA) system (SCRUM Inc., Tokyo, Japan) was developed for analysis of cell migration, invasion, and adhesion *in vitro*[7,8]. This system uses impedance detection to create a cell index that is used for continuous monitoring of cell viability, migration, and invasion[7,8]. In a previous study using RTCA we showed that EGCG inhibited cell migration and invasion in oral squamous cell carcinomas (OSCCs)[9]. Moreover, we have demonstrated that anaplastic thyroid cancer (ATC) cells (TCO-1) have high migratory and invasive activity in association with high periostin expression[10]. In particular, TCO-1 cells exhibit very high periostin expression compared with other cell lines tested[10].

ATC is a rare and highly malignant form of thyroid cancer with a high mortality rate[11]. Treatment of ATC is very difficult and consequently the survival rate is very low for associated head and neck cancers. At present, new therapeutic agents for ATC are in great demand.

Periostin, the expression of which is elevated in TCO-1 cells, was originally identified as an 811-amino acid protein secreted by osteoblasts[12]. Periostin has frequently been observed as a major constituent of the extracellular milieu of desmoplastic malignant tumors[13]. Periostin functions as a ligand for $\alpha_V\beta_3$ and $\alpha_V\beta_5$ integrins to support the adhesion and migration of ovarian epithelial cells[12]. However, few studies have examined the relationship between EGCG and periostin.

Integrins permit dynamic bidirectional transmembrane signaling that is essential in cell adhesion, migration, differentiation, and survival. Human integrins have 18 α- and 8 β-subunits that combine to give 24 different $\alpha\beta$ heterodimers[14]. Iwamoto *et al* reported that talin binding conformationally activates transmembrane integrin adhesion receptors to increase their affinity for extracellular ligands and promotes integrin clustering for high-affinity adhesion to the extracellular matrix[14]. Several studies have reported that EGCG inhibits the invasion and migration of cancer cells by suppressing the activation and expression of integrins[9,15,16]. It is thought that EGCG plays an important role in suppressing cancer metastasis by inhibiting integrins.

Previously, we reported on the inhibition of the migration and invasion of OSCCs using the RTCA system[9]. Moreover, we reported that TCO-1 cells exhibit a strong migratory activity compared with OSCCs. On the basis of these observations, we surmised that TCO-1 cells possess strong adhesive activity. In the present study, we used RTCA to investigate EGCG inhibition of the adhesion of an ATC cell line, as well as that of cell lines from cancers of the tongue and the floor of the mouth, and also the associated expression of periostin and integrin mRNA.

Materials and methods

Cell lines and reagents

All three cell lines used in the present study were provided by the Health Science Research Resources Bank (Osaka, Japan). TCO-1 (JCRB0239) cells were established from a human non-differentiated thyroid cancer[17], the SAS (JCRB0260) cell line was established from poorly

differentiated OSCC of the tongue[18], and the HO-1-u-1 cell line (JCRB0828) was established from a poorly differentiated OSCC of the floor of the mouth[19]. EGCG (MW458.37) was purchased from Wako Pure Chemical Industries (Osaka, Japan).

Cell culture

All cell lines were cultured at 37°C in humidified atmosphere of 5% CO_2 and 95% air in medium containing 10% fetal bovine serum (FBS), 100 U / ml penicillin, and 100 μg / ml streptomycin. TCO-1 cells were cultured in Dulbecco's modified Eagle's medium (DMEM), whereas SAS and HO-1-u-1 cells were cultured in 45% DMEM-45% Ham's F12 medium (DMEM / F12). The medium was changed every 3 days[10, 17-19].

Hematoxylin-eosin staining

After 6 h culture in the presence or absence of EGCG, TCO-1 cells were stained with hematoxylin-eosin (HE).

Real-time cell analysis

Previous studies have reported on the migration and invasion of OSCC cells as determined by RTCA[7, 9, 10]. In the present study, adhesion was assessed on an RTCA system E-Plate 16 coated with fibronectin (20 mg / ml). TCO-1 cells (1.5×10^4), SAS or HO-1-u-1 cells (1.0×10^5) were seeded onto an individual E-Plate 16s in 100 μL medium specific for each cell line without FBS. The final EGCG concentration in the TCO-1 medium was 10, 30, 50, 100, or 200 μM, whereas the final EGCG concentration in the SAS and HO-1-u-1 medium was 50, 100, or 200 μM. Changes in impedance resulting from cells that had migrated to the bottom side of the membranes were recorded every 15 min and were monitored for a total of 24 h.

A unitless parameter, termed the cell index (CI), was used to measure the relative change in electrical impedance as a marker of cell status. The CI is a relative and dimensionless value because it represents the impedance change divided by a background value.

RNA isolation and quantitative real-time reverse transcription-polymerase chain reaction

Head and neck cancer cells were seeded in six-well plates and grown for 1 week at 37°C. Total RNA was extracted using NucleoSpin RNA II (MACHEREY-NAGEL, Duren, Germany) after treatment with EGCG for 6 h. Total RNA was reverse transcribed using the PrimeScript RT Master Mix (TaKaRa Bio, Shiga, Japan). The resulting cDNAs were amplified using primers designed with ProbeFinder software (Roche Applied Science, Mannheim, Germany) for *periostin*, *α_1 integrin* (*ITGA1*), *ITGAV*, and *ITGB1*. Table 1 lists the primers used, the Roche Universal Probe Library probe numbers, and the gene accession numbers. Amplification was performed with a LightCycler (Roche) using the LightCycler TaqMan Master mix (Roche). The PCR reaction parameters were as follows: 95°C for 10 min, followed by 45 cycles (except for *18s* rRNA amplification = 25 cycles) of 10 s at 95°C, 30 s at 60°C, and 1 s at 72°C. Fluorescence data were analyzed using LightCycler software (Roche). mRNA levels of the genes of inter-

Table 1. Nucleotide sequences of primers used for polymerase chain reaction

Gene		Sequence	Accession number	Probe number
Periostin	Sense primer	5'-caccaaggtcaccaaattcat-3'	NM_001135934.1	#9
	Antisense primer	5'-ttcctcacgggtgtgtctc-3'		
ITGA1	Sense primer	5'-aattggctctagtcaccattgtt-3'	NM_181501.1	#14
	Antisense primer	5'-caaatgaagctgctgactggt-3'		
ITGAV	Sense primer	5'-gccgtggatttcttcgtg-3'	NM_002210.3	#64
	Antisense primer	5'-gaggacctgccctccttc-3'		
ITGB1	Sense primer	5'-cgatgccatcatgcaagt-3'	NM_002211.3	#65
	Antisense primer	5'-acaccagcagccgtgtaac-3'		
18s	Sense primer	5'-gcaattattccccatgaacg-3'	X03205.1	#48
	Antisense primer	5'-gggacttaatcaacgcaagc-3'		

ITG, integrin.

est were normalized against those of *18s* rRNA used as an internal standard to yield relative expression ratios[7].

Statistical analysis

The normal distribution of baseline variables for all data was evaluated using the Bonferroni test following one-way analysis of variance (ANOVA). All data are expressed as the mean ± SEM. $P < 0.05$ was considered significant.

Results

Fig. 1 shows HE-stained TCO-1 cells after 6 h culture in the absence (control) or presence of 200 μM EGCG. No obvious morphological changes (rounding and swelling) were observed after culturing cells in the presence of EGCG. There was no clear evidence of apoptosis or necrosis after culture in the presence of 200 μM EGCG. Similarly, EGCG did not induce apoptosis or necrosis in SAS and HO-1-u-1 cells (data not shown).

RTCA results of up to 6 h reflect changes in adhesion, whereas results after the 6-h time point reflect changes in cellular proliferation. Fig. 2 shows the effects of EGCG on cell adhesion (0–6 h) and proliferation (6–24 h) on the fibronectin-coated E-Plate 16s. EGCG inhibited TCO-1 adhesion in a concentration-dependent manner (Fig. 2A). After incubation with EGCG for 5 h, the CI for control, 30, 50, and 200 μM EGCG-treated TCO-1 cells was 5.80 ± 0.40, 3.33 ± 0.34, 0.68 ± 0.08, and 0.22 ± 0.02, respectively, with significant reductions in the CI in the presence of EGCG at all concentrations tested ($P < 0.01$ vs control for all). EGCG (50 μM) treatment resulted in a 97.8% inhibition of cell proliferation for up to 24 h (Fig. 2A). The adhesion of SAS cells was significantly decreased by 96.6% after 5 h exposure to 200 μM EGCG ($P < 0.01$ vs control and 50 μM EGCG), by 43.9% after 5 h exposure to 100 μM EGCG ($P < 0.01$ vs control and 50 μM EGCG), and by 8.92% after 5 h exposure to 50 μM EGCG ($P > 0.05$ vs

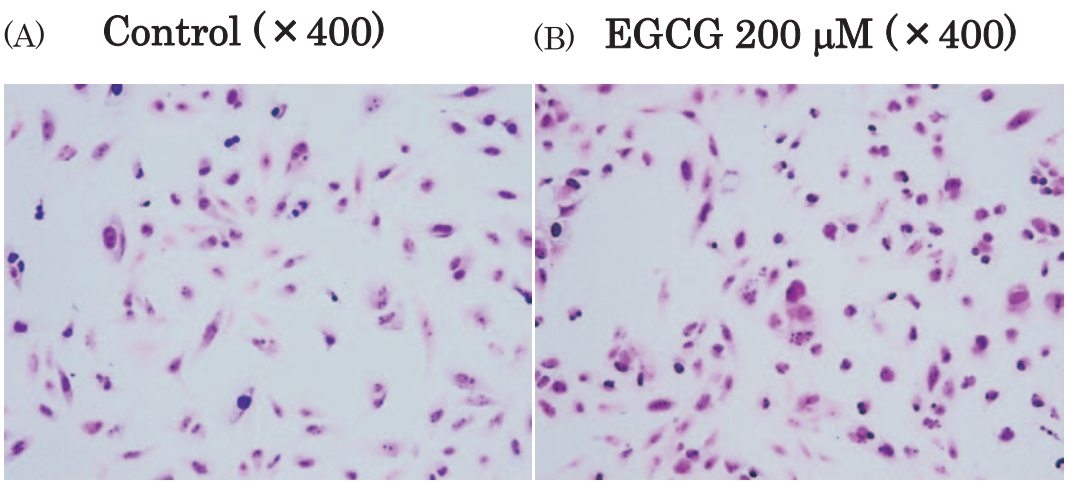

Fig. 1. Hematoxylin–eosin (HE) staining. TCO-1 cells were fixed in 10% formaldehyde for 1 h and were evaluated for morphological changes after 6 h culture in the presence of 200 μM (−)-epigallocatechin-3-gallate (EGCG) under an optical microscope after HE staining.

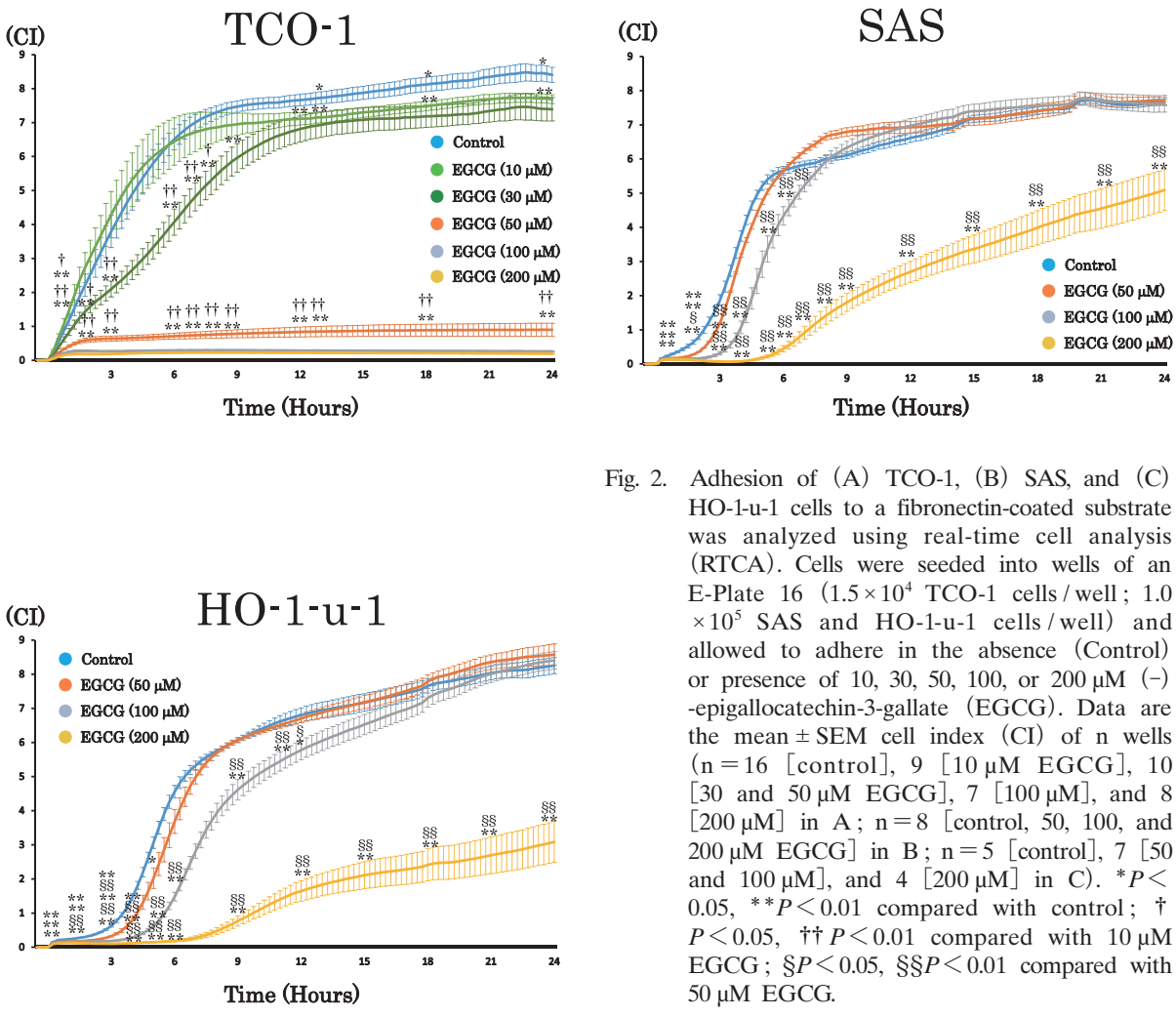

Fig. 2. Adhesion of (A) TCO-1, (B) SAS, and (C) HO-1-u-1 cells to a fibronectin-coated substrate was analyzed using real-time cell analysis (RTCA). Cells were seeded into wells of an E-Plate 16 (1.5×10^4 TCO-1 cells / well; 1.0×10^5 SAS and HO-1-u-1 cells / well) and allowed to adhere in the absence (Control) or presence of 10, 30, 50, 100, or 200 μM (−)-epigallocatechin-3-gallate (EGCG). Data are the mean ± SEM cell index (CI) of n wells (n = 16 [control], 9 [10 μM EGCG], 10 [30 and 50 μM EGCG], 7 [100 μM], and 8 [200 μM] in A; n = 8 [control, 50, 100, and 200 μM EGCG] in B; n = 5 [control], 7 [50 and 100 μM], and 4 [200 μM] in C). $^*P < 0.05$, $^{**}P < 0.01$ compared with control; †$P < 0.05$, ††$P < 0.01$ compared with 10 μM EGCG; §$P < 0.05$, §§$P < 0.01$ compared with 50 μM EGCG.

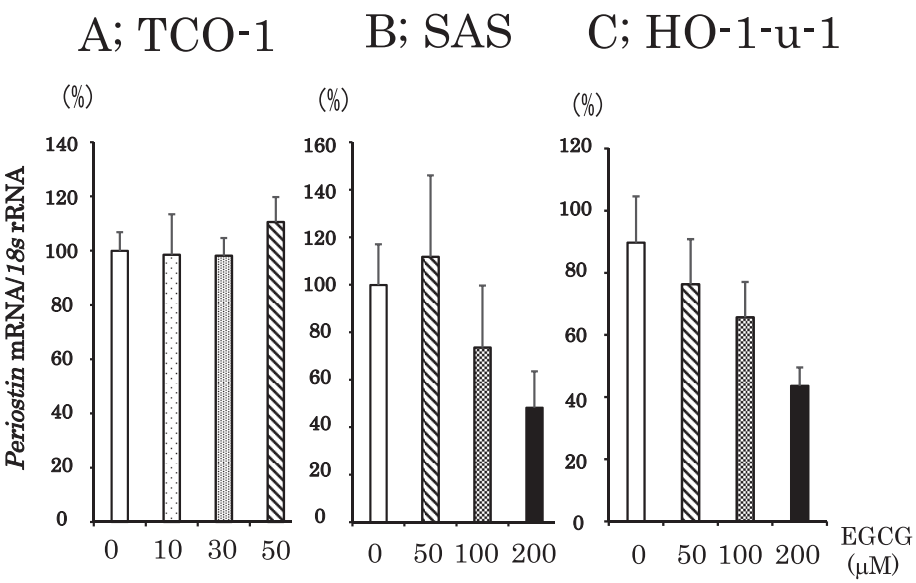

Fig. 3. *Periostin* mRNA expression in the absence or presence of (−)-epigallocatechin-3-gallate (EGCG) was determined using quantitative real-time polymerase chain reaction in (A) TCO-1, (B) SAS, and (C) HO-1-u-1 cells and is shown relative to that in the absence of EGCG. Data are the mean ± SEM (n = 12 [0 μM; Control], 12 [10 μM], 12 [30 μM], and 12 [50 μM] in A; n = 9 [0 μM], 5 [50 and 100 μM], and 6 [200 μM] in B; n = 10 [0 μM], 6 [50 and 100 μM], and 5 [200 μM] in C).

control; Fig. 2B). The adhesion of HO-1-u-1 cells was decreased by 95.2% after 5 h exposure to 200 μM EGCG ($P < 0.01$ vs control and 50 μM EGCG), by 79.8% after 5 h exposure to 100 μM EGCG ($P < 0.01$ vs control and 50 μM EGCG), and by 34.0% after 5 h exposure to 50 μM EGCG ($P < 0.05$ vs control; Fig. 2C). There were no clear effects of EGCG on the proliferation of HO-1-u-1 and SAS cells.

Fig. 3 shows *periostin* mRNA expression in head and neck cancer cells after 6 h exposure to EGCG. In these experiments, control expression was set at 100%. EGCG had no significant effect on *periostin* mRNA levels in TCO-1 cells (Fig. 3A), but there was a tendency for decreases in *periostin* mRNA levels in SAS and HO-1-u-1 cells after exposure to EGCG compared with control (Fig. 3B, C).

Fig. 4–6 show *ITGA1*, *ITGAV*, and *ITGB1* mRNA expression in head and neck cancer cells after 6 h treatment with EGCG. In these experiments, control expression was set at 100%. EGCG had no significant effect on *ITGA1* mRNA levels in TCO-1 (Fig. 4A), SAS (Fig. 4B), or HO-1-u-1 (Fig. 4C) cells. Treatment of TCO-1 cells with 30 and 50 μM EGCG resulted in a 61.3% and 9.8% decrease in *ITGAV* mRNA levels, respectively, compared with control ($P < 0.05$ vs 30 μM EGCG and $P < 0.01$ vs 50 μM EGCG; Fig. 5A). Treatment of SAS cells with 50, 100, and 200 μM EGCG resulted in a 59.7%, 52.5%, and 59.8% decrease in *ITGAV* mRNA levels, respectively, compared with control ($P < 0.01$ for all; Fig. 5B). Similarly, EGCG (50, 100, and 200 μM) treatment of HO-1-u-1 cells decreased *ITGAV* mRNA expression by 56.8%, 41.0%,

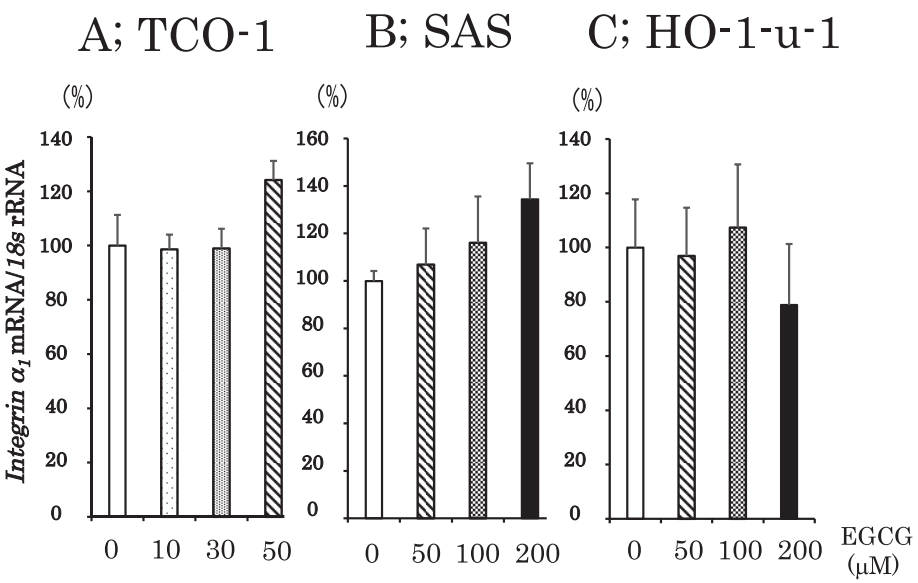

Fig. 4. *ITGA1* mRNA expression in the absence or presence of (−)-epigallocatechin-3-gallate (EGCG) was determined using quantitative real-time polymerase chain reaction in (A) TCO-1, (B) SAS, and (C) HO-1-u-1 cells and is shown relative to that in the absence of EGCG. Data are the mean ± SEM (n = 6 [0 μM] and 6 [10, 30, and 50 μM] in A; n = 9 [0 μM] and 6 [50, 100, and 200 μM] in B; n = 9 [0 μM] and 6 [50, 100, and 200 μM] in C).

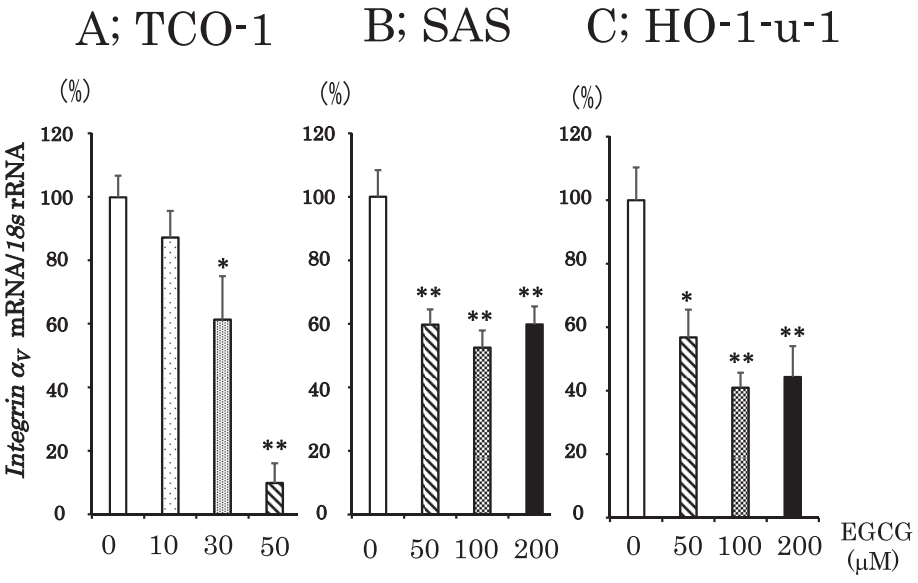

Fig. 5. *ITGAV* mRNA expression in the absence or presence of (−)-epigallocatechin-3-gallate (EGCG) was determined using quantitative real-time polymerase chain reaction in (A) TCO-1, (B) SAS, and (C) HO-1-u-1 cells and is shown relative to that in the absence of EGCG. Data are the mean ± SEM (n = 6 [0 μM] and 6 [10, 30, and 50 μM] in A; n = 18 [0 μM], 15 [50 and 100 μM], and 14 [200 μM] in B; n = 6 [0 μM] and 9 [50, 100, and 200 μM] in C). $^{*}P < 0.05$, $^{**}P < 0.01$ compared with 0 μM.

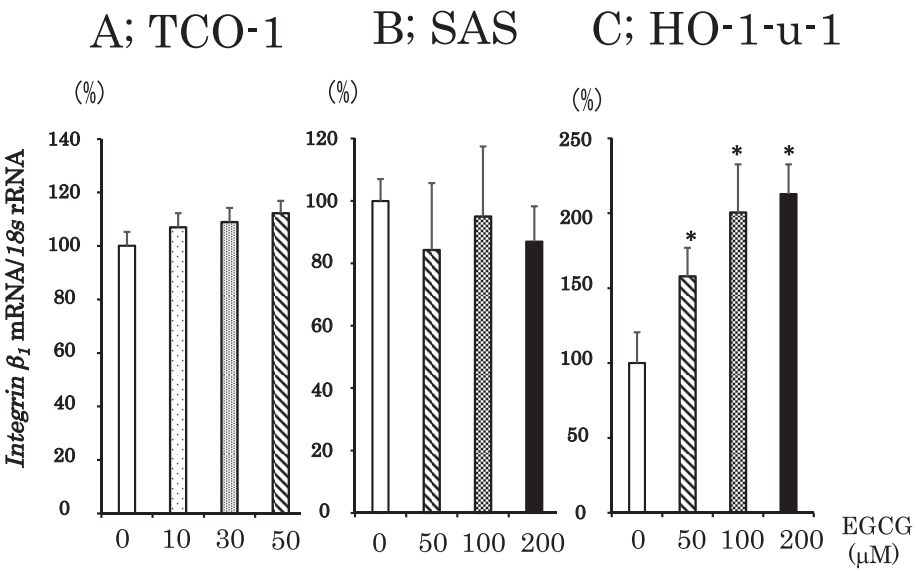

Fig. 6. *ITGB1* mRNA expression in the absence or presence of (−)-epigallocatechin-3-gallate (EGCG) was determined using quantitative real-time polymerase chain reaction in (A) TCO-1, (B) SAS, and (C) HO-1-u-1 cells and is shown relative to that in the absence of EGCG. Data are the mean ± SEM (n = 6 [0, 10, 30, and 50 μM] in A; n = 12 [0 μM], 6 [50 and 100 μM], and 5 [200 μM] in B; n = 9 [0 μM] and 6 [50, 100, and 200 μM] in C). $^*P < 0.05$ compared with 0 μM.

and 44.4%, respectively, compared with control ($P < 0.05$ vs 50 μM EGCG and $P < 0.01$ vs 100 μM and 200 μM EGCG; Fig. 5C). EGCG had no significant effect on *ITGB1* mRNA levels in TCO-1 (Fig. 6A) or SAS (Fig. 6B) cells. However, treatment of HO-1-u-1 cells with 50, 100, and 200 μM EGCG resulted in a 157.8%, 200.5%, and 212.7% increase in *ITGB1* mRNA levels, respectively, compared with control ($P < 0.05$ for all; Fig. 6C).

Discussion

In the present study, RTCA was used to demonstrate that EGCG inhibited the adhesion of ATC and poorly differentiated OSCC cell lines in real time and that these responses were associated with changes in the expression of α_V *integrin* but not *periostin*. The use of RTCA facilitated the identification of the effects of EGCG on three types of head and neck cancer cells, demonstrating significant inhibition of cell adhesion by EGCG.

Prominent extracellular matrix (ECM) proteins include fibronectin, laminin, and collagens. These proteins are deeply involved in tumor growth, invasion, and metastasis because of adhesive interactions between tumor cells and the ECM[20]. Using fibronectin-coated E-Plate 16s in the present study revealed that EGCG directly inhibited cancer cell interactions with fibronectin. Moreover, Suzuki *et al* reported that EGCG binds β_1 integrin[21]. Therefore, EGCG strongly and directly inhibits the binding of cells to the ECM. Moreover, RTCA indicated that EGCG inhibited the adhesion of all cells in a concentration-dependent manner. In particular, EGCG inhibited TCO-1 cell adhesion and proliferation. The findings of the present study show that at

100 and 200 μM, EGCG prevents the adhesion of TCO-1 cells to the surface of the plate. It is important to note that the CI is not altered by the presence of cells on the surface of the plate in the absence of adhesion[22,23]. Lim and Cha reported that EGCG (50–200 μM) inhibited cell proliferation and induced apoptosis in an ATC cell line (ARO cells) via suppression of the epidermal growth factor receptor (EGFR) / extracellular signal-regulated kinase (ERK) pathway and cyclin B1 / CDK1 complex[24]. However, in the present study, 200 μM EGCG did not induce apoptosis in TCO-1 cells.

Clinical studies of periostin expression in human cancers have found that increased expression of periostin is correlated with tumor metastasis[25,26]. Gillan *et al* reported that periostin promotes adhesion and potentiates cancer cell motility through binding to $\alpha_V\beta_3$ and $\alpha_V\beta_5$ integrins[12]. However, in the present study, EGCG did not decrease the expression of *periostin* mRNA in TCO-1 cells, and only 50 μM EGCG reduced α_V *integrin* mRNA expression in TCO-1 cells by 90%. Yan and Shao reported that cellular adhesion of 293T cells required signaling through $\alpha_V\beta_5$ integrin[27]. Therefore, EGCG suppresses adhesion of TCO-1 cells regardless of the overexpression of *periostin* observed in our previous study[10].

ATC is a very aggressive solid tumor with a poor prognosis. Surgery, radiotherapy, and chemotherapy do not improve the mean survival time, which is in the range of 2–6 months[28]. EGCG may become a potential treatment for ATC that cannot be otherwise treated effectively. Previous studies have demonstrated that one consumption of green tea extract (1.5–4.5 g or 1–3 cups) by healthy individuals results in plasma concentrations of EGCG of only 4 μM[29]. The ingestion of benifuuki tea, which contains *O*-methylated catechin, results in higher EGCG blood concentrations and may have a more beneficial effect than other green teas[30]. It is necessary to devise an effective means to administer EGCG, such as *O*-methylated EGCG, because it will be difficult to immediately use EGCG in a clinical setting.

In conclusion, using RTCA technology we clearly showed that EGCG inhibited the adhesion and proliferation responses of an ATC cell line in real time. The findings of the present study suggest that EGCG may be a lead compound for reducing the metastases of ATC by inhibiting integrins.

Conflict of interest disclosure

The authors declare they have no potential conflicts of interest.

References

1) Higdon JV, Frei B. Tea catechins and polyphenols: health effects, metabolism, and antioxidant functions. *Crit Rev Food Sci Nutr*. 2003;**43**:89–143.

2) Masuda S, Maeda-Yamamoto M, Usui S, *et al*. 'Benifuuki' green tea containing *O*-methylated catechin reduces symptoms of Japanese cedar pollinosis: a randomized, double-blind, placebo-controlled trial. *Allergol Int*. 2014;**63**:211–217.

3) Oka Y, Iwai S, Amano H, *et al*. Tea polyphenols inhibit rat osteoclast formation and differentiation. *J Pharmacol Sci*. 2012;**118**:55–64.

4) Balentine DA, Wiseman SA, Boumens LC. The chemistry of tea flavonoids. *Crit Rev Food Sci Nutr*. 1997;**37**:693-704.
5) Katiyar SK, Mukhtar H. Tea antioxidants in cancer chemoprevention. *J Cell Biochem Suppl*. 1997;**27**:59-67.
6) Cao Y, Cao R. Angiogenesis inhibited by drinking tea. *Nature*. 1999;**398**:381.
7) Ono T, Iwai S, Egawa S, *et al*. Investigation of cell migration and invasion using real-time cell analysis, as well as the association with matrix metalloproteinase-9 in oral squamous cell carcinomas. *Showa Univ J Med Sci*. 2013;**25**:203-212.
8) Atienza JM, Yu N, Kirstein SL, *et al*. Dynamic and label-free cell-based assays using the real-time cell electronic sensing system. *Assay Drug Dev Technol*. 2006;**4**:597-607.
9) Egawa S, Iwai S, Iijima K, *et al*. Quantification of (-)-epigallocatechin-3-gallate inhibition of migration and invasion of oral squamous cell carcinoma cell lines using real-time cell analysis. *Showa Univ J Med Sci*. 2015;**27**:71-81.
10) Hayashi T, Iwai S, Egawa S, *et al*. Quantification of migration and invasion and the association with periostin in anaplastic thyroid cancer using a real-time cell analyzer. *Showa Univ J Med Sci*. 2015;in press.
11) Ranganath R, Shah MA, Shah AR. Anaplastic thyroid cancer. *Curr Opin Endocrinol Diabetes Obes*. 2015;**22**:387-391.
12) Gillan L, Matei D, Fishman DA, *et al*. Periostin secreted by epithelial ovarian carcinoma is a ligand for alpha (V) beta (3) and alpha (V) beta (5) integrins and promotes cell motility. *Cancer Res*. 2002;**62**:5358-5364.
13) Sirica AE, Almenara JA, Li C. Periostin in intrahepatic cholangiocarcinoma: pathobiological insights and clinical implications. *Exp Mol Pathol*. 2014;**97**:515-524.
14) Iwamoto DV, Calderwood DA. Regulation of integrin-mediated adhesions. *Curr Opin Cell Biol*. 2015;**36**:41-47.
15) Park JH, Yoon JH, Kim SA, *et al*. (-)-Epigallocatechin-3-gallate inhibits invasion and migration of salivary gland adenocarcinoma cells. *Oncol Rep*. 2010;**23**:585-590.
16) Pilorget A, Berthet V, Luis J, *et al*. Medulloblastoma cell invasion is inhibited by green tea (-)epigallocatechin-3-gallate. *J Cell Biochem*. 2003;**90**:745-755.
17) Higashi T, Sasai H, Suzuki F, *et al*. Hamster cell line suitable for transfection assay of transforming genes. *Proc Natl Acad Sci U S A*. 1990;**87**:2409-2413.
18) Kitamura R, Toyoshima T, Tanaka H, *et al*. Association of cytokeratin 17 expression with differentiation in oral squamous cell carcinoma. *J Cancer Res Clin Oncol*. 2012;**138**:1299-1310.
19) Hayashi K, Yokozaki H, Naka K, *et al*. Effect of 9-*cis*-retinoic acid on oral squamous cell carcinoma cell lines. *Cancer Lett*. 2000;**151**:199-208.
20) Suzuki Y, Isemura M. Inhibitory effect of epigallocatechin gallate on adhesion of murine melanoma cells to laminin. *Cancer Lett*. 2001;**173**:15-20.
21) Suzuki Y, Suzuki T, Minami T, *et al*. Involvement of impaired interaction with β_1 integrin in epigallocatechin gallate-mediated inhibition of fibrosarcoma HT-1080 cell adhesion to fibronectin. *J Health Sci*. 2006;**52**:103-109.
22) Coffman FD, Cohen S. Impedance measurements in the biomedical sciences. *Anal Cell Pathol (Amst)*. 2012;**35**:363-374.
23) Emori H, Iwai S, Ryu K, *et al*. A new method for measuring osteoclast formation by electrical impedance. *J Pharmacol Sci*. 2015;**128**:87-91.
24) Lim YC, Cha YY. Epigallocatechin-3-gallate induces growth inhibition and apoptosis of human anaplastic thyroid carcinoma cells through suppression of EGFR/ERK pathway and cyclin B1/CDK1 complex. *J Surg Oncol*. 2011;**104**:776-780.
25) Sasaki H, Dai M, Auclair D, *et al*. Serum level of the periostin, a homologue of an insect cell adhesion molecule, as a prognostic marker in nonsmall cell lung carcinomas. *Cancer*. 2001;**92**:843-848.
26) Sasaki H, Dai M, Auclair D, *et al*. Serum level of the periostin, a homologue of an insect cell adhesion molecule, in thymoma patients. *Cancer Lett*. 2001;**172**:37-42.

27) Yan W, Shao R. Transduction of a mesenchyme-specific gene periostin into 293T cells induces cell invasive activity through epithelial–mesenchymal transformation. *J Biol Chem*. 2006;**281**:19700–19708.
28) Zito G, Richiusa P, Bommarito A, *et al*. In vitro identification and characterization of CD133 (pos) cancer stem-like cells in anaplastic thyroid carcinoma cell lines. *PLoS One* (Internet). 2008;**3**:e3544. (accessed 2016 Jan 20) Available from: http://journals.plos.org/plosone/article?id=10.1371/journal.pone.0003544
29) Irie Y, Iwai S, Amano H, *et al*. (−)-Epigallocatechin-3-gallate inhibits differentiation and matrix metalloproteinases expression in osteoclasts. *Showa Univ J Med Sci*. 2014;**26**:63–74.
30) Maeda-Yamamoto M, Ema K, Monobe M, *et al*. Epicatechin-3-*O*-(3″-*O*-methyl)-gallate content in various tea cultivars (*Camellia sinensis* L.) and its in vitro inhibitory effect on histamine release. *J Agric Food Chem*. 2012;**60**:2165–2170.

[Received January 8, 2016 : Accepted January 21, 2016]